Laser-induced fluorescence detection of lead atoms in a laser-induced plasma: an experimental analytical optimization study

Laville, Stéphane; Goueguel, Christian; Loudyi, Hakim; Vidal, François; Chaker, Mohamed; Sabsabi, Mohamad

Publisher's version / Version de l'éditeur:
https://doi.org/10.1016/j.sab.2009.03.021
Spectrochimica Acta Part B: Atomic Spectroscopy, 64, 4, pp. 347-353, 2009-04

SAB-03950; No of Pages 7

Spectrochimica Acta Part B xxx (2009) xxx–xxx

Contents lists available at ScienceDirect

Spectrochimica Acta Part B

journal homepage: www.elsevier.com/locate/sab

Laser-induced fluorescence detection of lead atoms in a laser-induced plasma: An experimental analytical optimization study

Stéphane Laville [a,*], Christian Goueguel [b], Hakim Loudyi [b], François Vidal [b], Mohamed Chaker [b], Mohamad Sabsabi [a]

[a] National Research Council of Canada, Industrial Materials Institute, 75 de Mortagne Blvd., Boucherville, Québec, Canada J4B 6Y4
[b] INRS Énergie, Matériaux et Télécommunications, 1650 Boul. Lionel Boulet, Varennes, Québec, Canada H3C 3J7

ARTICLE INFO

Article history:
Received 27 May 2008
Accepted 29 March 2009
Available online xxxx

Keywords:
Laser-induced breakdown spectroscopy
Laser-induced fluorescence
Lead
Enhanced sensibility
Limit of detection

ABSTRACT

The combination of the laser-induced breakdown spectroscopy (LIBS) and laser-induced fluorescence (LIF) techniques was investigated to improve the limit of detection (LoD) of trace elements in solid matrices. The influence of the main experimental parameters on the LIF signal, namely the ablation fluence, the excitation energy, and the inter-pulse delay, was studied experimentally and a discussion of the results was presented. For illustrative purpose we considered detection of lead in brass samples. The plasma was produced by a Q-switched Nd:YAG laser and then re-excited by a nanosecond Optical Parametric Oscillator (OPO) laser. The experiments were performed in air at atmospheric pressure. We found out that the optimal conditions were obtained for our experimental set-up using relatively weak ablation fluence of 2–3 J/cm^2 and an inter-pulse delay of about 5–10 μs. Also, a few tens of microjoules was typically required to maximize the LIF signal. Using the LIBS–LIFS technique, a single-shot LoD for lead of about 1.5 part per million (ppm) was obtained while a value of 0.2 ppm was obtained after accumulating over 100 shots. These values represent an improvement of about two orders of magnitude with respect to LIBS.

1. Introduction

Over the recent years, the LIBS (laser-induced breakdown spectroscopy) technique has become an important tool for real-time spectrochemical analysis of a wide variety of materials. Indeed, it offers many advantages over most of the other existing techniques: no sample preparation is required, a stand-off and *in situ* real-time analysis is possible, multi-element measurements can be performed on solids, liquids and gases, and damage to the samples are minimized since only a few micrograms of the sample is usually required for the analysis. However, a conclusion often drawn from the literature about the LIBS technique is its poorer sensitivity in comparison with other consolidated, but more cumbersome, analytical techniques [1,2].

Up to now, several approaches have been proposed to improve the limit of detection (LoD) achievable using LIBS. One of the most promising options consists in using two successive laser pulses instead of only one as in conventional LIBS. In the so-called "double-pulse LIBS" approach [3–10] the second pulse is used to globally reheat the plasma generated by the first pulse with perpendicular or collinear configuration. The most studied combinations in the "double-pulse LIBS" approach are: (i) same pulse duration and wavelength for both pulses [4–7], (ii) mixed-pulse duration (different pulse durations but same wavelength) [8,9] and (iii) mixed-wavelength (different wavelengths but same duration) [10]. In the "double-pulse LIBS" approach, the improvement of the LoD was shown to be generally less than one order of magnitude. Among the approaches based on the use of two successive laser pulses, the combination of LIBS with LIFS (laser-induced fluorescence spectroscopy) has been shown to be the most promising to reduce significantly the LoD.

The LIBS–LIFS approach (sometimes also denoted LIBS-LEAFS — LIBS combined with Laser-Excited Atomic Fluorescence Spectroscopy) consists in generating a plasma using a first laser pulse and then populating a specific quantum level of the trace element of interest using a second laser pulse tuned on a specific wavelength. The subsequent fluorescence signal emitted from this level is used for analytical studies. The LIBS–LIFS approach has already been shown to enable the detection of trace elements in the ppb range. In addition, the calibration curves generally exhibit linearity over several orders of magnitude in concentration. Hence, apart from a greater technical complexity, the LIBS–LIFS approach displays the same advantages as the single-pulse LIBS but offers a much higher sensitivity and selectivity.

Although the LIFS technique has been intensively studied experimentally and theoretically (see for instance, [11–14]), relatively few papers have been devoted to its combination with LIBS [16–29]. Up to now, the LIBS–LIFS approach has already been successfully applied to the detection of various trace elements in liquids [16–18], aerosols [19]

* Corresponding author. Tel.: +1 450 641 5230; fax: +1 450 641 5106.
E-mail addresses: Stephane.Laville@cnrc-nrc.gc.ca (S. Laville), Gouegel@emt.inrs.ca (C. Goueguel), Loudyi@emt.inrs.ca (H. Loudyi), Vidal@emt.inrs.ca (F. Vidal), Chaker@emt.inrs.ca (M. Chaker), Mohamad.Sabsabi@cnrc-nrc.gc.ca (M. Sabsabi).

0584-8547/$ – see front matter © 2009 Published by Elsevier B.V.
doi:10.1016/j.sab.2009.03.021

and solids [20–29] in ambient air or under various controlled atmospheres. For instance, Gornushkin et al. [20] have demonstrated LoDs of 1, 0.2 and 20 ppm, accumulating over 10 laser shots, for the analysis of cobalt in soils, graphite and steels, respectively, in air at atmospheric pressure. In [21], the same group also reported a LoD of 72 ng/g (72 ppb) for lead in copper, accumulating over 2000 shots, under a low pressure argon atmosphere. In [22], LoDs of 0.3 μg/g (300 ppb) and 0.5 μg/g (500 ppb) have been achieved for cadmium and thallium, respectively, in soils, accumulating over 30 shots. These values were two orders of magnitude lower than those obtained using LIBS in optimum conditions. In [23], Sdorra et al. have demonstrated LoDs for silicon, chromium and boron in steels of 600 ng/g (600 ppb), 4 μg/g (4 ppm) and 9 μg/g (9 ppm), respectively (the two first values were obtained over 30 shots while the last one is the single-shot value). Snyder et al. [24] reported LoDs of 0.2 and 0.5 ppm, accumulating over 50 shots, for the detection of lead and bismuth in copper, respectively. In [25], single-shot LoDs obtained for chromium and silicon in steel samples were 105 and 95 ppm, respectively, instead of 270 and 300 ppm in LIBS. Smith et al. also applied LIBS–LIFS to the measurement of isotope ratios for lithium [26] and uranium [27] under a low pressure atmosphere and accumulating over 200 shots. In [28], LIBS–LIFS was applied to the detection of chromium in different parts of the human body and the single-shot LoD was improved by a factor 6, from 120 to 20 ppm, when compared to LIBS.

Although all these investigations clearly demonstrate the great potential of the LIBS–LIFS technique for reducing the LoD, the majority of the published works was devoted to optimizing the LoD for a dedicated application and very little was done to understand the plasma conditions to be achieved to optimize the signal-to-noise ratio (SNR) of the LIF signal emitted by the re-excited atoms.

The goal of this paper is to present a parametric investigation of the SNR and discuss the main physical parameters involved in LIFS applied to the particular context of laser-produced plasmas. For that purpose we focused on the detection of lead in brass samples. After optimization, we achieved a LoD of about two orders of magnitude smaller than with LIBS. The main experimental parameters investigated here are: (i) the laser excitation energy, (ii) the ablation laser fluence, and (iii) the delay between ablation and excitation laser pulses. We also discuss the choice of the acquisition delay and the gate width.

2. Experimental

A schematic of our experimental set-up is shown in Fig. 1. The ablation was carried out using a Q-switched Nd:YAG laser (Continuum, Surelite II) that can deliver up to 600 mJ per pulse at a wavelength of 1064 nm. The pulse duration was $\tau = 7$ ns at full width half maximum (FWHM). The ablation beam was focused onto the target by a plano-convex BK7 lens (25.4-mm diameter, $f = 25$ cm focal length) at normal incidence to the target. The spot diameter onto the surface of the samples was about 2 mm. The ablation was performed in air at atmospheric pressure and the repetition rate was 2 Hz to prevent any interaction between the laser and aerosols. Finally, the ablation fluence (F_{ABL}) was varied from 1.6 to 4.8 J/cm^2.

The 2nd laser pulse was delivered by an Optical Parametric Oscillator (OPO) laser (Continuum, Panther). The synchronization of the two laser pulses was achieved using an 8-channel programmable delay generator (model 565, Berkeley Nucleonics Corporation). The OPO pulse duration was 7 ns and the repetition rate was 10 Hz. The OPO was pumped by a 355 nm frequency tripled Q-switched Nd:YAG laser with energy limited to about 250 mJ per pulse. At the various outputs of the OPO (doubled signal or idler, signal and idler — see Fig. 1), the wavelength of the laser pulse can be tuned from 215 nm to 2.7 μm and the corresponding energy ranges from 10 μJ (at about 320 nm) to 70 mJ (at about 450 nm). The excitation energy was adjusted using a set of neutral density filters and measured using a low energy pyroelectric detector (Ophir, PE10).

The light emitted by the plasma was collected by an optical fiber positioned next to the plasma plume and connected to the entrance slit of a Czerny–Turner spectrometer (VM 504, Acton Research). Its focal length is 0.39 m while its f-number is 5.4. It was equipped with a 1200 lines/mm (blazed at 150 nm) grating that leads to a linear dispersion of about 2.1 nm/mm. The spectrometer was coupled with an ICCD detector (Istar DH720-25H-05, Andor) containing 1024×256 pixels of dimensions 26 μm^2. The width of the intensified acquisition window was about 56 nm and the spectral resolution was

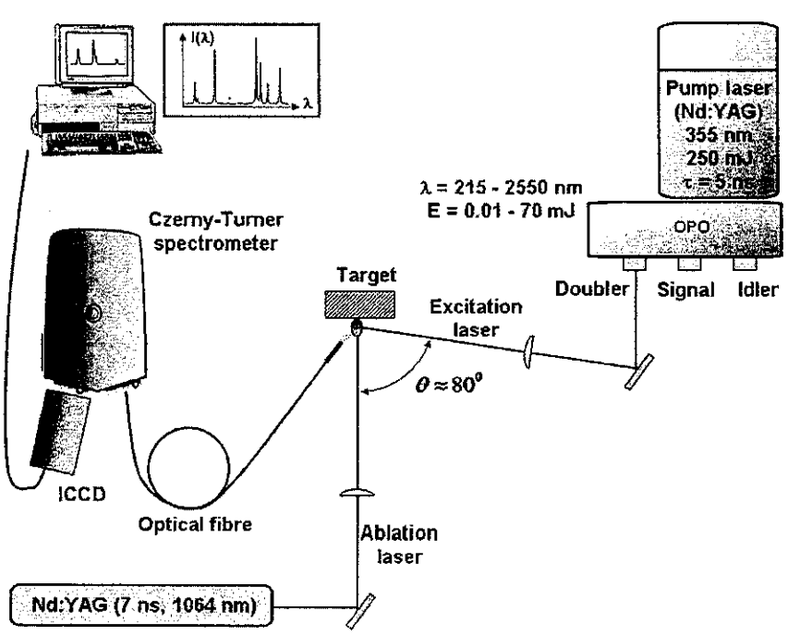

Fig. 1. Schematic of the experimental set-up.

Please cite this article as: S. Laville, et al., Laser-induced fluorescence detection of lead atoms in a laser-induced plasma: An experimental analytical optimization study, Spectrochim. Acta Part B (2009), doi:10.1016/j.sab.2009.03.021

about 0.16 nm. A long wave pass filter was positioned at the input of the spectrometer to filter the scattered radiation of the OPO laser.

Since the OPO spot (ellipse of 8×15 mm) was much larger than the plasma plume (typically a few mm^2 in air at atmospheric pressure [34]), we focused the beam using a plano-convex fused silica lens (25.4-mm diameter, $f=20$ cm focal length) down to an area of about 2 mm^2, which achieved a reasonable spatial overlap with the plasma plume. The OPO energy was varied from a few tenth of μJ to several hundreds of μJ, corresponding to a maximum fluence of a few tens of mJ/cm^2, which is much lower than the damage threshold of metals for nanosecond pulses [30].

This set-up was used to measure small amounts of lead in brass samples. The targets used here are 10 certified brass samples whose certified concentrations of Cu and Pb are given in Table 1 (these samples were calibrated standards as provided by Alcan (Canada), CTIF (France) or SUS (Germany)).

The laser excitation and fluorescence decay scheme used in this study for the detection of lead is illustrated in Fig. 2. Lead atoms were excited by the OPO laser, tuned at 283.31 nm, from the ground level $6\ ^3P_0$ (denoted 0) to the $7\ s\ 3P_1^0$ level (denoted m) located at 35,287.24 cm^{-1}. The subsequent fluorescence signal associated with the spontaneous decay from the $7\ s\ 3P_1^0$ level to the $6\ ^3P_2$ level (denoted n) at 10,650.47 cm^{-1} was then observed at 405.78 nm.

For each sample, 100 spectra were acquired at each of 4 positions on the sample with a 1 mm inter-site distance in order to get a sufficiently representative sampling and account for any eventual lack of spatial homogeneity. Also, 300 cleaning shots were performed prior any acquisition to avoid the contribution of surface contaminants. The samples were translated using a double axis motorized stage (Newport, UTM 100 mm) equipped with a programmable controller (Newport, model ESP 300).

3. Results and discussion

The SNR of the LIF signal emitted by the excited lead atoms depends essentially on: i) the excitation wavelength (λ_{EXC}), ii) the excitation fluence (F_{EXC}), iii) the ablation fluence (F_{ABL}), iv) the angle between the normal to the surface of the sample and the excitation beam (θ), v) the delay between the ablation and excitation pulses or inter-pulse delay (Δt_{IP}), the acquisition delay (t), i.e., the time when the fluorescence signal starts to be integrated, and finally vi) the integration gate width (Δt). It is worth pointing out that in LIF, the irradiance is generally used to characterize the excitation laser instead of the fluence, since the excitation rate is the key parameter. However, the fluence was preferred here because it is more customary in LIBS literature. Both quantities are equivalent when the pulse duration and its temporal shape are kept constant.

The influence of the angle θ was not studied here due to geometrical constraints in our set-up and was set to $\theta=80°$, as shown in Fig. 1. The influence of this parameter has however already been discussed in [28] where the best SNR was obtained for angles θ in the range of 80–90°, justifying our choice here.

Table 1
Reduced composition of our set of certified brass samples.

Sample number	Cu (% weight)	Pb (ppm)
1	95.50	30
2	98.40	30
3	99.7785	50
4	99.7622	90
5	97.0	190
6	99.7207	290
7	99.6502	510
8	95.67	560
9	98.668	800
10	81.12	1100

Only concentrations of Pb and Cu are shown.

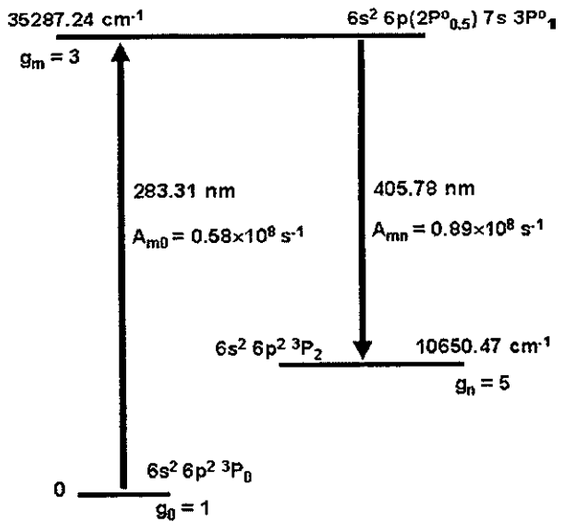

Fig. 2. Reduced energy level diagram of lead. Only the levels and transitions involved in our experiments are shown.

Regarding the temporal parameters t and Δt, we found out experimentally that the LIF signal was observable from the arrival of the excitation beam into the plasma and typically lasted approximately 10 ns, which is on the order of both the laser pulse duration (7 ns) and the fluorescence decay time $1/A_{mn}=3.7$ ns for the Pb(I) 405.78 nm line. In our experiments, we set the acquisition delay a few ns before the inter-pulse delay Δt_{IP} in order to avoid any jitter, and the gate width to $\Delta t=40$ ns in order to acquire the entire fluorescence signal.

In our conditions, the LIF signal was maximized for an entrance slit width of 350 μm. It is worth pointing out that the spectral resolution is generally not a critical issue in LIBS–LIFS since the LIF signal is sufficiently brief so that the signal of possible neighbor strong lines is negligible compared to the LIF signal. This specificity is of great interest for line-rich spectra where spectral interferences limit sometimes the performances of LIBS.

In the following we investigated the influence of the remaining experimental parameters λ_{EXC}, F_{EXC}, F_{ABL} and Δt_{IP} on the SNR (or the LIF signal itself) for the Pb(I) 405.78 nm line.

3.1. Influence of the experimental parameters

The influence of the major experimental parameters on the LIF signal emitted by lead atoms was investigated using sample number 6 (Section 3.1.1 and 3.1.3). Samples 2 and 10 were added when studying the influence of the excitation fluence (Sec. 3.1.2).

Although the influence of the excitation wavelength and fluence on the LIF signal has been thoroughly studied in the context of flames, discharges and ICP plasmas (see for instance, [11–15,33,34]), these parameters have been much less studied in LIBS plasmas, which differ in many respects (fast time evolution, higher temperature, etc.) from those media. For this reason, the influence of these two parameters has been investigated in this paper.

3.1.1. Influence of the OPO wavelength

Fig. 3 shows the LIF signal of the Pb(I) 405.78 nm line averaged over 100 acquisition shots as a function of the wavelength of the excitation pulse delivered by the OPO laser. The other parameters were $F_{ABL}=3.2$ J/cm^2, $\Delta t_{IP}=5$ μs and $F_{EXC}=10$ mJ/cm^2, that were similar to the optimum conditions found in the following. One can see in Fig. 3 that the LIF signal is centered on the excited Pb(I) 283.31 nm line and that the FWHM of the spectral distribution is about 80 pm.

Please cite this article as: S. Laville, et al., Laser-induced fluorescence detection of lead atoms in a laser-induced plasma: An experimental analytical optimization study, Spectrochim. Acta Part B (2009), doi:10.1016/j.sab.2009.03.021

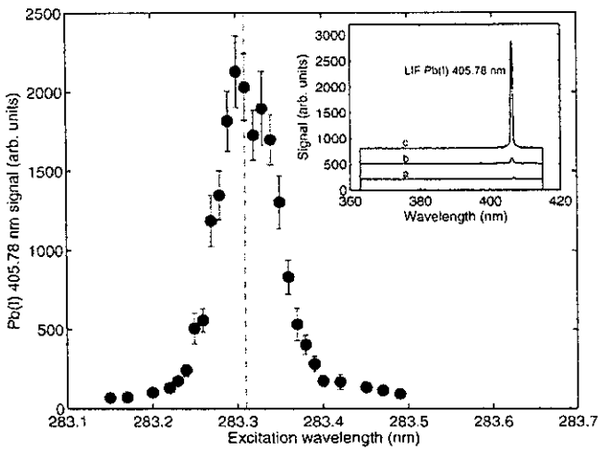

Fig. 3. LIF signal of the Pb(I) 405.78 nm line as a function of the excitation wavelength delivered by the OPO laser – the inset shown the LIBS–LIFS spectra averaged over 100 shots obtained in different experimental conditions. a: without OPO, b: when the OPO is tuned slightly off-resonance ($\lambda = 282.85$ nm) and finally c: when the OPO is on-resonance ($\lambda = 283.31$ nm). The spectra a, b and c were shifted vertically for better readability.

which is much larger than the line width of the OPO laser, estimated as about 18 pm.

The line width observed in Fig. 3 is likely not due to Stark broadening, which is generally the main broadening mechanism in plasmas. As a matter of fact, estimating the electron density as about 10^{16} cm^{-3} at 5 μs (using the properties of aluminum [31], which are not expected to differ significantly from those of copper), and using the Stark broadening coefficient $w = 7\times10^{-3}$ nm for the Pb(I) 405.78 nm line [32], one obtains a FWHM of $\Delta\lambda_{1/2} \approx 14$ pm. The observed profile width is likely due to saturation broadening (see for instance [14,33,34]), which is a consequence of the above-saturation fluence used to populate the level m. Using the formulas derived in [34] for a 2-level system (which can be shown to be the same for a 3-level system) and assuming a Lorentzian line profile, the FWHM is given by $\Delta\lambda_{1/2}\sqrt{1 + F_{EXC}/F_{EXC}^{SAT}}$ where F_{EXC}^{SAT} is the saturation value of the excitation fluence. In our operating conditions, the ratio F_{EXC}/F_{EXC}^{SAT} was 40 since the saturation fluence was estimated as $F_{EXC}^{SAT} \approx 0.25$ mJ/cm^2 for sample 6, as discussed below, so that $\Delta\lambda_{1/2} \approx 90$ pm which is in better agreement with the measured one.

The inset of Fig. 3 shows three LIBS–LIFS spectra, averaged over 100 acquisition shots, obtained in the following conditions: (a) without OPO laser, (b) when the OPO laser is tuned slightly off-resonance (282.85 nm), and (c) when the OPO laser is on-resonance (283.31 nm). One observes that without the OPO laser the Pb(I) 405.78 nm line is hardly discernible from the background. When getting closer to resonance, this line becomes clearly observable until it reaches the maximum at the resonance.

Fig. 3 clearly demonstrates that the absorption of the 2nd pulse is mainly a resonant process and is not taking place through inverse Bremsstrahlung such as in "double-pulse LIBS." Such a resonant absorption is only possible for sufficiently long delays and weak ablation fluences as discussed below. In the following, the excitation wavelength was maintained to 283.31 nm in order to maximize the LIF signal.

3.1.2. Influence of the excitation fluence

Fig. 4 shows the Pb LIF signal at 405.78 nm as a function of the excitation fluence F_{EXC}, generally known as the saturation curve. The results are presented for samples denoted 2, 6 and 10 in Table 1, containing 30, 290 and 1100 ppm of Pb, respectively. The other parameters were $F_{ABL} = 2.4$ J/cm^2 and $\Delta t_{IP} = 8$ μs.

The two distinct regimes usually observed in LIFS experiments (as well as in LIBS–LIFS experiments for detection of traces of Fe [16] and Li [26]) can be seen in Fig. 4: for weak excitation fluences, the LIF signal evolves linearly with the excitation fluence while for high fluences, the LIF signal tends to saturate (the so-called optical saturation regime). We have fitted the measurements of Fig. 4 with the following expression [12,14]:

$$I_F = I_F^{SAT}\frac{F_{EXC}}{F_{EXC}^{SAT} + F_{EXC}} \quad (1)$$

where I_F^{SAT} is the saturated value of the LIF signal and F_{EXC}^{SAT} is the saturation fluence, which are 0.14, 0.25 and 0.53 mJ/cm^2 for samples 2, 6 and 10, respectively. The poor quality of the fits shown in Fig. 4 are likely due to the fact that Eq. (1) holds in specific conditions that are not strictly satisfied here. For example, the steady-state condition [11–13] is likely not satisfied in our experiments since $A_{mn}\tau$ is not much greater than one, assuming that collisional processes are negligible. In addition, the condition of homogeneity of the laser beam and the medium, discussed in [14,15], does probably not hold here since the OPO laser was focused inside the plasma. Other effects that can distort the saturation curve are also discussed in [14].

One also observes in Fig. 4, that the ratios of the saturated LIF signals for the various samples approximately follow the lead concentration ratios, i.e., a ratio of ~8.1 between samples 6 and 2 and a ratio of ~3.4 between samples 10 and 6. However, these ratios are not respected for low excitation fluences since, in particular, the LIF signals from samples 6 and 10 are hardly distinguishable, considering the error bars. This behavior is reflected in the fitted values of the saturation fluence F_{EXC}^{SAT} in Eq. (1), which differ for the three samples considered.

This result, which seems to be in contradiction with the generally admitted principle that the LIF signal is proportional to the concentration of emitters for all fluences, is probably due to the fact that our plasmas are not optically thin, as discussed below (LIF in optically thick media was also discussed in [14] and [15] for instance).

The plasma can be said optically thin if:

$$\sigma_{0m} N_{Pb} / S_p \lesssim 1 \quad (2)$$

where σ_{0m} is the photon absorption cross section, N_{Pb} is the number of Pb atoms in the plasma, and S_p is the area of plasma (assumed to be completely illuminated by the OPO laser for simplicity) which is

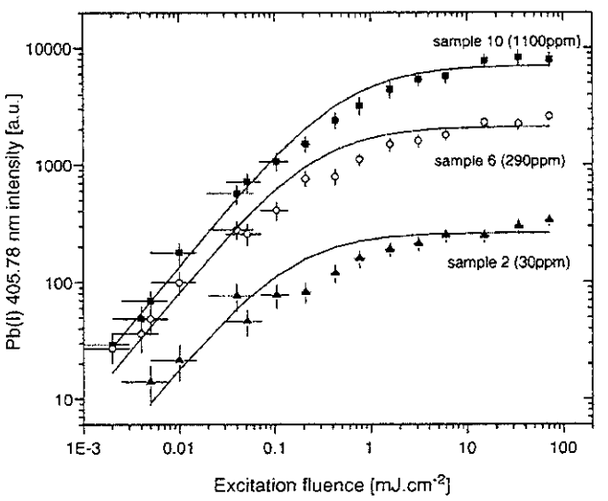

Fig. 4. LIF signal of Pb(I) 405.78 nm line as a function of the excitation fluence. The results are shown for sample 2 (30 ppm), 6 (290 ppm) and 10 (1100 ppm). The curves result from a fit using Eq. (1) (stationary case for a 3-level system).

Please cite this article as: S. Laville, et al., Laser-induced fluorescence detection of lead atoms in a laser-induced plasma: An experimental analytical optimization study, Spectrochim. Acta Part B (2009), doi:10.1016/j.sab.2009.03.021

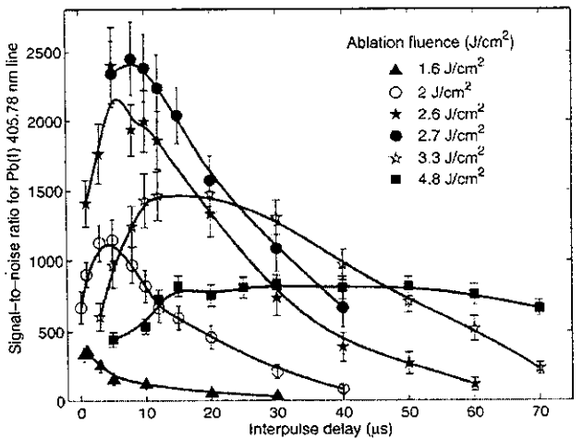

Fig. 5. Signal-to-noise ratio for the Pb(I) 405.78 nm line as a function of the inter-pulse delay for several ablation fluences.

generally on the order of the mm^2 several microseconds after the plasma formation [31]. In order to check if Eq. (2) is verified in the cases considered in Fig. 4, we estimated the photon absorption cross section at the center of the line as [35]:

$$\sigma_{0m} = \frac{c\lambda_{0m}^4 g_m A_{m0}}{4\pi^2 c g_0 \Delta\lambda_{1/2}} \tag{3}$$

where $\Delta\lambda_{1/2}$ is the FWHM of the excitation line without the excitation laser. Assuming that the line is mainly broadened by the Stark effect, which we estimate as 14 pm, as discussed above, one finds $\sigma_{0m} \approx 1.4 \times 10^{-13}$ cm^2. To estimate the value of N_{Pb}, the ablated depth was measured using low coherence interferometry (LCI) that provides the profile of the ablation crater (more details about this technique can be found in [36]). The ablation rate was estimated to about $h = 30$ nm per shot using a fluence of 2.4 J/cm^2 (the ablation crater, used in the measurement of h resulted from 5000 successive laser shots). Therefore, since the ablation crater diameter was about 2 mm, one finds that about 0.8 μg of matter was ablated per laser shot. One then concludes that $N_{Pb} \approx 10^{11}$ for sample number 2, and therefore, $\sigma_{0m} N_{Pb} \approx 1$ mm^2. For the reasonable value of $S_p \approx 2$ mm × 2 mm [31] one can see that Eq. (2) is verified for sample 2, but not for samples 6 and 10, for which $\sigma 0_m N_{Pb}$ is equal to ~10 mm^2 and ~30 mm^2, respectively.

When the plasma becomes optically thick, i.e., $\sigma_{0m} N_{Pb}/S_p \gg 1$, and when the fluence is below saturation, all the incident photons are absorbed and the number of excited atoms is nearly equal to the number of incident photons. Therefore, the LIF signal below saturation does not depend on the Pb concentration, a fact that is nearly verified in Fig. 4 for samples 6 and 10. However, at saturation, the fluence is high enough to excite all the Pb atoms, and the LIF signal is thus proportional to the Pb concentration, as observed in Fig. 4.

From these considerations, one concludes that understanding all the features of Fig. 4 would require not only a time-dependent 3-level model (possibly taking collisions into account) but also a model taking into account the depletion of the laser pulse propagating into the plasma. In addition, this model should take account of self-absorption of the fluorescence signal in optically thick plasmas for fluences below saturation. Such a model was however beyond the scope of this paper.

3.1.3. Influence of ablation fluence and inter-pulse delay

Fig. 5 shows the SNR for the Pb(I) 405.78 nm line as a function of the inter-pulse delay (Δt_{IP}) for several ablation fluences (F_{ABL}). The excitation fluence was 10 mJ/cm^2, which means that the optical saturation regime was achieved, as shown in Fig. 4. For calculating the SNR, the CCD dark current noise, that is the primary source of noise, was evaluated on spectral region free of lines. B-splines functions were added as a visual aid to illustrate the trends in the data.

The main feature of Fig. 5 is that the SNR reaches a maximum at inter-pulse delays which depends somewhat on the ablation fluence. Similar behaviors have been observed in the detection of Fe in water [16], of Si in steels [23] and of Pb in lead nitrate aerosols [19].

The behavior observed in Fig. 5 can be interpreted as follows. For small inter-pulse delays the plasma temperature is maximum, i.e., typically several electron-volts in our conditions [31], so that most Pb atoms are excited or ionized, and the ground level ($^3P_0$) is weakly populated. Consequently, the excitation pulse is marginally absorbed by the few Pb atoms in the ground state. In addition, the quenching collisions rate is expected to be higher at high temperature since electron density and velocity are higher. As the inter-pulse delay increases, the plasma temperature decreases due to plasma expansion and radiative cooling. Therefore, the Pb population in the ground level increases and the quenching collisions rate decreases (as electrons recombine and slow down), leading to higher absorption of the excitation beam and thus higher LIF signal. However, for very long inter-pulse delays the coupling between the excitation beam and the plasma volume becomes less efficient since fewer Pb atoms are intercepted by the excitation beam, leading to the decrease observed in Fig. 5.

The dependence on the ablation fluence F_{ABL} seen in Fig. 5 is made clearer in Fig. 6, which shows the same data as Fig. 5 but plotted as a function of F_{ABL} for several inter-pulse delays Δt_{IP}. When the ablation fluence is weak, i.e., close to the ablation threshold F_{ABL}^{th}, the amount of ablated matter is small. Consequently, the LIF signal, which depends on the number of ablated Pb atoms, is weak (from [37], the value of F_{ABL}^{th} is about 1.5 J/cm^2 for a 7 ns laser pulse at 1064 nm, a value which is consistent with Figs. 5 and 6). As the ablation fluence increases, the amount of ablated Pb atoms that can be excited by the OPO laser beam increases, and so the LIF signal. However, for a given inter-pulse delay Δt_{IP}, the plasma temperature increases as the fluence increases, so that fewer Pb atoms are available in the ground state and the quenching collisions rate is higher. Fig. 6 also shows that the maximum SNR appears for higher ablation fluences when the inter-pulse delay increases. This can be explained by the fact that higher fluences produce higher initial temperatures and thus longer times are required to reach a value of the temperature for which the number of Pb atoms in the ground state is maximized.

From Figs. 5 and 6 one concludes that the LIF signal is optimal when the number of ablated lead atoms is large enough and when the

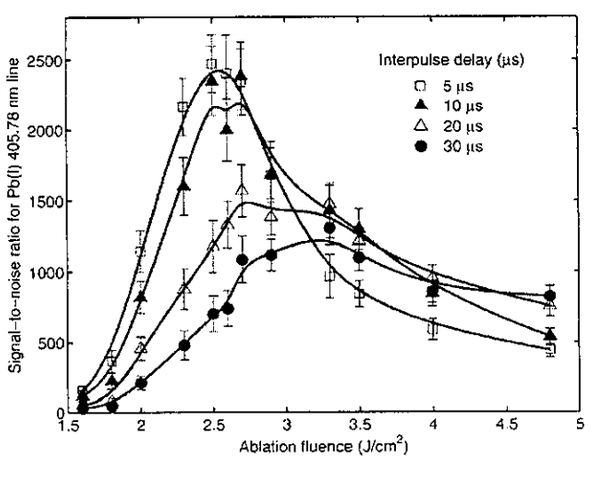

Fig. 6. Signal-to-noise ratio for the Pb(I) 405.78 nm line as a function of the ablation fluence for several inter-pulse delays.

Please cite this article as: S. Laville, et al., Laser-induced fluorescence detection of lead atoms in a laser-induced plasma: An experimental analytical optimization study, Spectrochim. Acta Part B (2009), doi:10.1016/j.sab.2009.03.021

temperature is low enough to maintain a significant fraction of them in the ground state and minimize the quenching collision rate.

3.2. LIBS–LIFS calibration curves and limit of detection

Fig. 7 shows the single-shot SNR for the Pb(I) 405.78 nm line as a function of lead concentration for the set of 10 calibration samples shown in Table 1. The results are presented for LIBS–LIFS but also for LIBS for an absolute comparison of both techniques. 100 acquisition shots per position were performed over 3 positions.

When using LIBS–LIFS, the ablation fluence, inter-pulse delay and excitation fluence were $F_{ABL} = 2.7$ J/cm^2, $\Delta t_{IP} = 8$ μs, and $F_{EXC} =$ 10 mJ/cm^2, respectively (as discussed earlier, this set of values enables maximizing the LIF signal). The LIBS–LIFS calibration curve shown in Fig. 7 exhibits a good linearity since the regression line passing through the origin (0, 0) is characterized by a correlation factor $r^2 = 0.981$ (the spread of the data could be mainly attributed to an insufficient sampling). It was also found in previous works that the LIBS–LIFS calibration curves display excellent linearity over several orders of magnitude in concentration. For instance, linearity was observed over four orders of magnitude for cobalt traces in graphite [20] and also for lead traces in copper [21].

The single-shot LoD resulting from Fig. 7 is about 1.5 ppm while an accumulation over 100 shots leads to a LoD of about 0.2 ppm. These values were calculated on the basis of the standard 3σ-convention, where σ is the standard deviation of the background noise. An estimation of the single-shot LoD based on the sample with the lowest Pb concentration (30 ppm – sample 1) in our set (i.e., through the expression $\text{LoD} = C_{Pb} \times 3/\text{SNR}$, where C_{Pb} is the Pb concentration of the sample and SNR is the corresponding signal-to-noise ratio) gives the close value of 0.7 ppm. Similar values have been obtained in LIBS–LIFS literature using the same excitation–fluorescence scheme. For instance, Snyder et al. have demonstrated a LoD of 0.5 ppm accumulating over 50 laser shots [24], while in [21] a LoD of 72 ng/g (72 ppb) was obtained over 2000 shots.

The results obtained using conventional LIBS from our experimental set-up are also shown in Fig. 7. The ablation fluence was about 41 J/cm^2 while the acquisition delay and the gate width were $t = 0.8$ μs and $\Delta t = 15$ μs, respectively. The slit width was 50 μm. Using the same 3σ-convention, we obtained a single-shot LoD of about 200 ppm, i.e., about two orders of magnitude higher than the value measured using LIBS–LIFS. Although the LIBS calibration curve exhibits a poor linearity ($r^2 = 0.911$), this value of the LoD is validated by the fact that the Pb(I) 405.78 nm line was not visible on the spectra obtained with samples containing less than about 200 ppm.

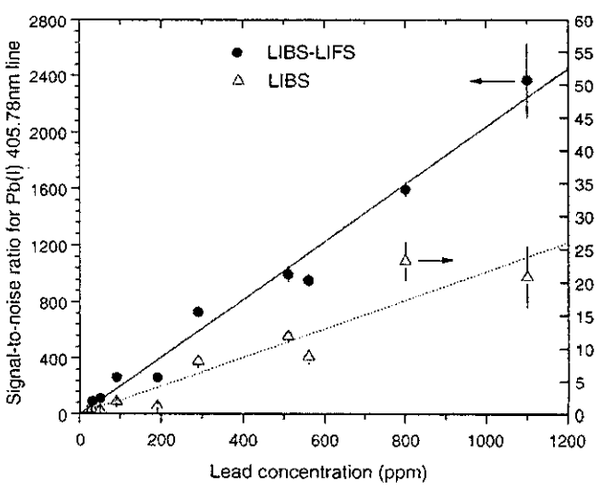

Fig. 7. Signal-to-noise ratio for the Pb(I) 405.78 nm line as a function of the lead concentration obtained using LIBS and LIBS–LIFS techniques.

4. Conclusion

In this paper, laser-induced breakdown spectroscopy (LIBS) combined with laser-induced fluorescence (LIF) was studied. The detection of lead traces in a copper matrix was chosen as an illustrative purpose. The goals here were to: (i) study the influence of the main experimental parameters on the LIF signal, (ii) identify optimum experimental conditions to maximize the LIF signal, and finally (iii) compare LIBS–LIFS to LIBS to evaluate the improvement in the LoD in the optimal conditions.

A parametric study was first conducted to investigate the influence of the main experimental parameters on the LIF signal. These parameters were: the ablation and excitation fluences and the inter-pulse delay. Using a sample containing 290 ppm of lead, an optimum set of experimental parameters was identified. For our particular set-up, an ablation fluence of 2.7 J/cm^2, an excitation fluence of few tens of mJ/cm^2 and an inter-pulse delay in the 5–8 μs range was shown to maximize the LIF signal. These figures would however, be different for a different overlap between the plasma and the excitation beam and possibly for a different collection system geometry. In the ideal case where all the emitters could be excited and their LIF signal collected, the optimum LIF signal would be obtained for very high ablation fluences and very long inter-pulse delays.

A physical interpretation of the influence of the plasma conditions and experimental parameters on the LIF signal has been given. It turns out that the main quantities to consider are: (i) the amount of ablated matter, (ii) the plasma temperature, (iii) the excitation fluence, and (iv) the interaction volume.

Using the optimum parameters found, a calibration curve for lead was produced using a set of 10 certified samples containing from 30 to 1100 ppm of lead. A single-shot limit of detection of about 1.5 ppm was achieved and this value was reduced to about 0.2 ppm after accumulation over 100 laser shots. This value is among the best reported in literature for solid targets and has be estimated to be about 2 orders of magnitude lower than obtained from usual LIBS.

The general conclusions drawn from this work on the role of the experimental parameters could also be, in principle, applied to the detection of other trace elements in the framework of the LIBS–LIFS technique. However, we do not believe that optimization of the remaining experimental parameters (mainly the angle of incidence of the excitation beam and the laser spot size) would dramatically change the results. In addition, further improvements in the experimental arrangement, that were beyond the scope of this paper, could be performed to reach even lower LoDs without accumulating over a larger number of shots. Indeed, the LoD depends critically on the optical collection system and the background noise of the detector. In this context, it is likely that the spectrometer/ICCD combination could be replaced by an interferential filter and a photomultiplier (PMT) to reduce light losses and increase the photon conversion efficiency.

Acknowledgments

The authors would like to acknowledge Bruno Gauthier at the IMI-NRC for the measurements of the ablation crater profiles, and Dr. N. Omenetto for fruitful discussions. This work was financially supported by the Natural Science and Engineering Research Council of Canada (NSERC).

References

[1] K. Meissner, T. Lippert, A. Wokaun, D. Guenther, Analysis of trace metals in comparison of laser-induced breakdown spectroscopy with LA-ICP-MS, Thin Solids Films 453–454 (2004) 316–322.

[2] P. Fichet, M. Tabarant, B. Sallé, C. Gauthier, Comparisons between LIBS and ICP/OES, Anal. Bioanal. Chem. 385 (2006) 338–344.
[3] V.I. Babushok, F.C. DeLucia, J.L. Gotfried, C.A. Munson, A.W. Miziolek, Double pulse laser ablation and plasma: laser induced breakdown spectroscopy signal enhancement, Spectrochim. Acta Part B 61 (2006) 999–1014.
[4] W. Pearman, J. Scaffidi, M. Angel, Dual-pulse laser-induced breakdown spectroscopy in bulk aqueous solution with an orthogonal beam geometry, Appl. Opt. 42 (30) (2003) 6085–6093.
[5] A. De Giacomo, M. Dell'Aglio, F. Colao, R. Fantoni, Double pulse laser produced plasma on metallic target in seawater: basic aspects and analytical approach, Spectrochim. Acta Part B 59 (2004) 1431–1438.
[6] L. St-Onge, M. Sabsabi, P. Cielo, Analysis of solids using laser-induced plasma spectroscopy in double-pulse mode, Spectrochim. Acta Part B 53 (1998) 407–415.
[7] D.N. Stratis, K.E. Eland, S.M. Angel, Dual-pulse LIBS using a pre-ablation spark for enhanced ablation and emission, Appl. Spectrosc. 54 (12) (2000) 1719–1726.
[8] J. Scaffidi, J. Pender, W. Pearman, S.R. Goode, B.W. Colston, J.C. Carter, S.M. Angel, Dual-pulse laser-induced breakdown spectroscopy with the combinations of femtosecond and nanosecond pulses, Appl. Opt. 42 (30) (2003) 6099–6106.
[9] J. Scaffidi, W. Pearman, J.C. Carter, S.M. Angel, Observations in collinear femtosecond–nanosecond dual pulse laser-induced breakdown spectroscopy, Appl. Spectrosc. 60 (1) (2006) 65–71.
[10] L. St-Onge, V. Detalle, M. Sabsabi, Enhanced laser-induced breakdown spectroscopy using the combination of fourth-harmonic and fundamental Nd:YAG laser pulses, Spectrochim. Acta Part B 57 (2002) 121–135.
[11] N. Omenetto, C.A. Van Dijk, J.D. Winefordner, Some consideration on the saturation parameter for 2- and 3-level systems in laser excited fluorescence, Spectrochim. Acta Part B 37 (1982) 703–711.
[12] D.R. Olivares, G.M. Hieftje, Saturation of energy levels in analytical atomic fluorescence spectrometry – I. Theory, Spectrochim. Acta Part B 33 (1978) 79–98.
[13] M.A. Bolshov, A.V. Zybin, V.G. Koloshnikov, K.N. Koshelev, Some characteristics of laser excited atomic fluorescence in a three-level scheme, Spectrochim. Acta Part B 32 (1977) 279–286.
[14] C.Th.J. Alkemade, Anomalous saturation curves in laser-induced fluorescence, Spectrochim. Acta Part B 40 (1985) 1331–1368.
[15] R.A. Van Calcar, M.J.M. Van De Ven, B.K. Van Uitert, K.J. Biewenga, T.J. Hollander, C. Th. Alkemade, Saturation of sodium fluorescence in a flame irradiated with a pulsed tunable dye laser, J. Quant. Spectrosc. Rad. Transfer 21 (1979) 11–18.
[16] M. Nakane, A. Kuwako, K. Nishizawa, H. Kimura, C. Konagai, T. Okamura, Analysis of trace metal elements in water using laser-induced fluorescence for laser-breakdown spectroscopy, Proc. SPIE 3935 (2000) 122–131.
[17] S. Koch, W. Garen, W. Neu, R. Reuter, Resonance fluorescence spectroscopy in laser-induced cavitation bubbles, Anal. Bioanal. Chem. 385 (2006) 312–315.
[18] Y. Godwal, S.L. Lui, M.T. Taschuk, Y.Y. Tsui, R. Fedosejevs, Determination of lead in water using laser ablation–laser induced fluorescence, Spectrochim. Acta Part B 62 (2007) 1443–1447.
[19] R.E. Neuhauser, U. Panne, R. Niessner, G.A. Petrucci, P. Cavalli, N. Omenetto, On-line and in-situ detection of lead aerosols by plasma-spectroscopy and laser-excited atomic fluorescence spectroscopy, Anal. Chim. Acta 346 (1997) 37–48.
[20] J.B. Gornushkin, J.E. Kim, B.W. Smith, S.A. Baker, J.D. Winefordner, Determination of Cobalt in soil, steel, and graphite using excited-state laser fluorescence induced in a laser spark, Appl. Spectrosc. 51 (1997) 1055–1059.
[21] I.B. Gornushkin, S.A. Baker, B.W. Smith, J.D. Winefordner, Determination of lead in metallic reference materials by laser ablation combined with laser excited atomic fluorescence, Spectrochim. Acta Part B 52 (1997) 1653–1662.
[22] F.H. Kortenbruck, R. Noll, P. Wintjens, H. Falk, C. Becker, Analysis of heavy metals in soils using laser-induced breakdown spectrometry combined with laser-induced fluorescence, Spectrochim. Acta Part B 56 (2001) 933–945.
[23] W. Sdorra, A. Quentmeier, K. Niemax, Basic investigations for laser microanalysis: II. Laser-induced fluorescence in laser-produced sample plumes, Mikrochim. Acta II 2 (4–6) (1989) 201–218.
[24] S.C. Snyder, J.D. Grandy, J.K. Partin, An investigation of laser-induced breakdown spectroscopy augmented by laser-induced fluorescence, ICALEO '98 Conference Proceeding 1998, Section C, 1998, p. 254, Orlando (FL).
[25] H.H. Telle, D.C.S. Beddows, G.W. Morris, O. Samek, Sensitive and selective spectrochemical analysis of metallic samples: the combination of laser-induced breakdown spectroscopy and laser-induced fluorescence spectroscopy, Spectrochim. Acta Part B 56 (2001) 947–960.
[26] B.W. Smith, I.B. Gornushkin, L.A. King, J.D. Winefordner, A laser ablation–atomic fluorescence technique for isotopically selective determination of lithium in solids, Spectrochim. Acta Part B 53 (1998) 1131–1138.
[27] B.W. Smith, A. Quentmeier, M. Bolshov, K. Niemax, Measurement of uranium isotope ratios in solid samples using laser ablation and diode laser-excited atomic fluorescence spectrometry, Spectrochim. Acta Part B 54 (1999) 943–958.
[28] O. Samek, M. Liska, J. Kaiser, V. Krzyzanek, Laser ablation for mineral analysis in the human body: integration of LIFS with LIBS, part of the EUROPTO conference on Biomedical Optical Systems and Laser-Assisted Biotechnology, SPIE Proc. 3570 (1998) 263–271.
[29] S. Laville, F. Vidal, M. Chaker, M. Sabsabi, Laser-Induced Breakdown Spectroscopy: Investigation of Pb Resonant Excitation and Decay Paths, Photonics North 2006 Conference SPIE, vol. 6343, 2006, 634321-1-8.
[30] B. Le Drogoff, F. Vidal, S. Laville, M. Chaker, T.W. Johnston, O. Barthélemy, J. Margot, M. Sabsabi, Laser-ablated volume and depth as a function of the pulse duration in aluminum targets, Appl. Opt. 44 (2005) 278–281.
[31] O. Barthélemy, J. Margot, M. Chaker, M. Sabsabi, F. Vidal, T.W. Johnston, S. Laville, B. Le Drogoff, Influence of the laser parameters on the space and time characteristics of an aluminum laser-induced plasma, Spectrochim. Acta Part B 60 (2005) 905–914.
[32] A. Alonso-Medina, Experimental determination of the Stark widths of Pb I spectral lines in a laser-induced plasma, Spectrochim. Acta Part B 63 (2008) 598–602.
[33] E.H. Piepmeier, Theory of laser saturated atomic resonance fluorescence, Spectrochim. Acta Part B 27 (1972) 431–443.
[34] N. Omenetto, J. Bower, J. Bradshaw, C.A. Van Dijk, J.D. Winefordner, A theoretical and experimental approach to laser saturation broadening in flames, J. Quant. Spectrosc. Radiat. Transfer 24 (1980) 147–158.
[35] A. Thorne, U. Litzén, S. Johansson, Spectrophysics Principles and Applications, Springer-Verlag, 1999.
[36] M.L. Dufour, G. Lamouche, V. Detalle, B. Gauthier, P. Sammut, Low-coherence interferometry – an advanced technique for optical metrology in industry, Insight 47 (4) (2005) 216–219.
[37] L.M. Cabalin, J.J. Laserna, Experimental determination of laser induced breakdown thresholds of metals under nanosecond Q-switched laser operation, Spectrochim. Acta Part B 53 (1998) 723–730.

Please cite this article as: S. Laville, et al., Laser-induced fluorescence detection of lead atoms in a laser-induced plasma: An experimental analytical optimization study, Spectrochim. Acta Part B (2009), doi:10.1016/j.sab.2009.03.021